Eur Biophys J (2003) 32: 519–528
DOI 10.1007/s00249-003-0296-9

ARTICLE

**Blaž Valič · Muriel Golzio · Mojca Pavlin
Anne Schatz · Cecile Faurie · Bruno Gabriel
Justin Teissié · Marie-Pierre Rols · Damijan Miklavčič**

Effect of electric field induced transmembrane potential on spheroidal cells: theory and experiment

Received: 10 June 2002 / Revised: 20 December 2002 / Accepted: 14 February 2003 / Published online: 24 April 2003

Abstract The transmembrane potential on a cell exposed to an electric field is a critical parameter for successful cell permeabilization. In this study, the effect of cell shape and orientation on the induced transmembrane potential was analyzed. The transmembrane potential was calculated on prolate and oblate spheroidal cells for various orientations with respect to the electric field direction, both numerically and analytically. Changing the orientation of the cells decreases the induced transmembrane potential from its maximum value when the longest axis of the cell is parallel to the electric field, to its minimum value when the longest axis of the cell is perpendicular to the electric field. The dependency on orientation is more pronounced for elongated cells while it is negligible for spherical cells. The part of the cell membrane where a threshold transmembrane potential is exceeded represents the area of electropermeabilization, i.e. the membrane area through which the transport of molecules is established. Therefore the surface exposed to the transmembrane potential above the threshold value was calculated. The biological relevance of these theoretical results was confirmed with experimental results of the electropermeabilization of plated Chinese hamster ovary cells, which are elongated. Theoretical and experimental results show that permeabilization is not only a function of electric field intensity and cell size but also of cell shape and orientation.

Keywords Chinese hamster ovary cells · Electroporation · Finite-element modelling · Spheroidal cells · Transmembrane potential

B. Valič · M. Pavlin · D. Miklavčič
Faculty of Electrical Engineering, University of Ljubljana, Trzaska 25, 1000 Ljubljana, Slovenia

M. Golzio · A. Schatz · C. Faurie · B. Gabriel
J. Teissié · M.-P. Rols (✉)
Institut de Pharmacologie et de Biologie Structurale du CNRS, UMR 5089, 205 Route de Narbonne, 31077 cedex Toulouse, France
Tel.: +33-5-61175811
Fax: +33-5-61175994

Abbreviations

Geometry a length of box side · d membrane thickness · $g_{\varphi\varphi}$ and $g_{\tau\tau}$ elements of metric tensor in spheroidal coordinates · $p(\vartheta)$ arc length on an ellipse · r_i vector of the point $T(x,y,z)$ lying at the surface of the spheroid · R cell radius in the case of a sphere · R_1, $R_2 = R_3$ axes of cell in the case of a spheroid (prolate spheroid: $R_1 > R_2 = R_3$; oblate spheroid $R_1 < R_2 = R_3$) · S area (surface) · T point at the surface of the spheroid · ρ ratio between R_1 and R_2 · ϑ, φ, r spherical coordinates · τ, φ, σ spheroidal coordinates
Electric E applied electric field · j_n normal component of electric current at the surface of the spheroid · L_i depolarizing factor in the $i = x$, y and z directions · α azimuth angle in the spherical coordinate system; the angle between the symmetry axis of the spheroid and the external electric field · β polar angle in the spherical coordinate system · ϕ electric potential · σ_i conductivity of cytoplasm · σ_o external medium conductivity · σ_m conductivity of cell membrane · $\Delta\phi$ transmembrane potential · $\Delta\phi_c$ threshold or critical transmembrane potential · $\Delta\phi_i$ induced transmembrane potential · $\Delta\phi_r$ resting transmembrane potential

Introduction

One of the developing techniques for introducing molecules which are deprived of membrane transport mechanisms in living cells is electropermeabilization, a method where the external electric field is used to permeabilize cell membranes and can be used for gene transfection (Neumann et al. 1982; Sukharev et al. 1992; Rols et al. 1998a; Satkauskas et al. 2002) and electrochemotherapy (Mir 2001). The study of induced transmembrane potentials in biological cells exposed to electromagnetic fields is important for improvement of these applications as well as for studying potential health effects of electric and magnetic fields (Fear and Stuchly 1998).

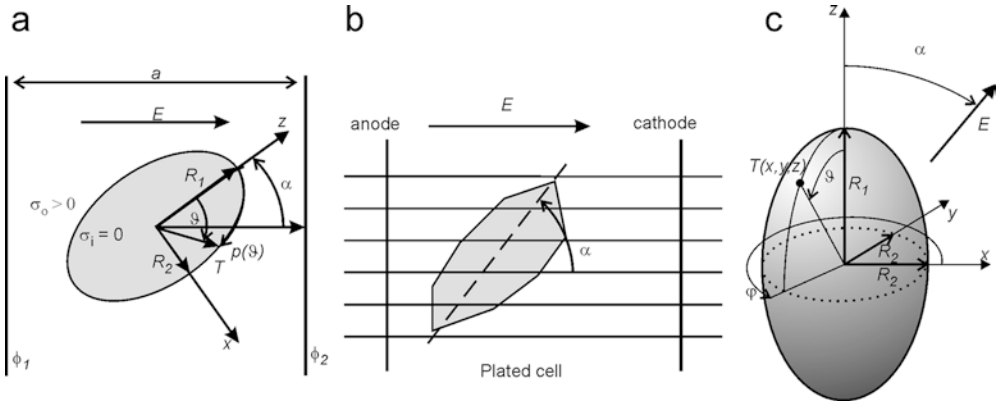

Fig. 1 Schematic representation of a spheroid (**a**) and plated CHO cell in the applied electric field (**b**). ϕ_1 and ϕ_2 are constant potentials, which are applied to induce a homogenous electric field. A cross-section of a spheroid with the xz plane is shown. α is the angle of orientation between the electric field and the z axis of symmetry and $p(\vartheta)$ is the arc length for a given angle ϑ. Spherical coordinates in the system of the spheroid are shown in (**c**)

When the electric field is applied to a cell, a change in transmembrane potential is induced on the cell membrane, which can cause biochemical and physiological changes of the cell. When the threshold value of the transmembrane potential is exceeded, the cell membrane becomes permeable, thus allowing entrance of molecules that otherwise cannot cross the membrane (Mir 2001). A further increase in the electric field intensity may cause irreversible membrane permeabilization and cell death. Thus the induced transmembrane potential ($\Delta\phi_i$) is a critical parameter for cell permeabilization. However, it was shown previously that the induced transmembrane potential is superimposed on the resting transmembrane potential ($\Delta\phi_r$) (Zimmerman 1982; Tekle et al. 1990; Teissié and Rols 1993). The absolute value of the threshold transmembrane potential ($\Delta\phi_c$) is in the range 200–1000 mV (Weaver and Powell 1989; Teissié and Rols 1993; Eynard et al. 1998; Bier et al. 1999; Miklavčič et al. 2000). Since in many cases $\Delta\phi_c$ can be considered to be much larger than $\Delta\phi_r$ (which is between −20 mV and −70 mV), we can to a first approximation ignore $\Delta\phi_r$. Nevertheless, we also evaluated the importance of taking into account both $\Delta\phi_i$ and $\Delta\phi_r$ for plated Chinese hamster ovary (CHO) cells in our calculations and showed that $\Delta\phi_r$ can indeed be neglected.

Induced transmembrane potential on a spheroid

The steady-state $\Delta\phi_i$ on a spherical cell is defined by Schwan's equation (Schwan 1957), which for ideal non-conductive membranes is:

$$\Delta\phi_i = \frac{3}{2} ER\cos\vartheta \tag{1}$$

where E is the applied electric field, R the cell radius and ϑ the angle defined between the applied electric field and the point vector of the calculation on the cell membrane.

Non-spherical cells can be approximated as prolate or oblate spheroids. To calculate $\Delta\phi_i$ on a spheroidal cell, some simplifications have to be made to solve the Laplace equation, i.e. a very thin membrane ($d << R_1$, R_2) and a low conductive membrane ($\sigma_m << \sigma_i$, σ_o). The solutions for parallel and perpendicular orientations are given in many papers (Fricke 1925; Schwartz et al. 1965; Bernhardt and Pauly 1973; Zimmermann et al. 1974; Hart and Marino 1982; Kotnik and Miklavčič 2000). From the solution of the Laplace equation (Sillars 1937; Stratton 1941) for the potential on an arbitrary oriented spheroid the $\Delta\phi_i$ values can be obtained for all orientations (Gimsa and Wachner 2001). The $\Delta\phi_i$ values for a non-conductive membrane can thus be written as a generalized Schwan equation (see Appendix A):

$$\Delta\phi_i = E\sin\alpha\frac{1}{1-L_x}x + E\cos\alpha\frac{1}{1-L_z}z \tag{2}$$

where L_x and L_z are depolarizing factors given in Appendix A (Eqs. 9 and 10) which depend only on the geometrical properties of the spheroid. The variables x and z are the coordinates of the point T on the surface of the spheroid (Fig. 1a and c) and E is the strength of the applied electric field. The angle α is the angle between the symmetry axis of the spheroid and the external electric field, as shown in Fig. 1, and defines the cell orientation with respect to the electric field.

To evaluate the influence of cell orientation on $\Delta\phi_i$, we calculated $\Delta\phi_i$ on a spheroidal cell for different orientations numerically, by using the finite elements method, and analytically according to Eq. 2. It was previously shown that electropermeabilization takes place only on the part of the cell membrane where $\Delta\phi_c$ is exceeded (Gabriel and Teissié 1998). Therefore, the surface with an overcritical $\Delta\phi$ has been calculated to determine the theoretical permeabilization. These results were then compared to the experimental results obtained by electropermeabilization of mammalian cells. CHO cells were used because of their spheroidal shape when attached to the substrate. The attached cells have different orientations with respect to the electric field direction (defined by the angle α; Fig. 1b) and do not reorient themselves under a short electric field application.

Materials and methods

Theoretical calculations

A finite elements model of a cell in a conducting medium was built for numerical analysis. For generation of models and calculations,

the program package Maxwell (Ansoft, Pittsburgh, Pa., USA) was used. Additional drawings and comparison between results were performed in Matlab (The MathWorks, Mass., USA).

The cell was modelled as a prolate ($R_1 > R_2 = R_3$) or oblate ($R_1 < R_2 = R_3$) spheroid. For cells that slightly differ from a spherical shape, a ratio between R_1 and R_2, $\rho = R_1/R_2 = 10/8$, was used. In the case of more elongated cells, the ratio $\rho = 10/5$ was used, corresponding to plated CHO cells, which are approximately 40 μm long and 20 μm wide. For bacilli a ratio of $\rho = 10/2$ and for erythrocytes a ratio of $\rho = 2/10$ were used. A bacillus is a 4 μm long and 0.8 μm wide prolate spheroid (Brock et al. 1984) and an erythrocyte is similar to a 2 μm long and 8 μm wide oblate spheroid (Miller and Henriqez 1988).

Under experimental conditions, however, plated CHO cells are more similar to half of a prolate spheroid lying on an insulating plate than to a whole prolate spheroid. However, for electrostatic or current flow modelling the insulating plate represents the mirroring plane boundary condition and thus the field distribution and consequentially the $\Delta\phi_i$ on the membrane are the same for the whole spheroidal cell as for half of the cell placed on the insulating plate.

For calculations we assumed steady-state conditions. This is justified, if the duration of the electric pulse (usually 0.1–10 ms) is long with respect to the time constant of the cell membrane polarization, which is in the range of microseconds (Neumann 1989; Kotnik et al. 1997). This was also the case in our experiments on electropermeabilization, where electric pulses of 5 ms duration were used.

To model an isolated cell we enclosed the spheroid in a box with side a five times longer than the cell largest radius. To estimate the error due to the finite dimension of the box, a box was used where a was eight times the longest radius. The observed difference was only around 1%. The box represents the external medium having conductivity σ_o. The cell was represented as a non-conductive object, since under physiological conditions the membrane conductivity is many orders smaller than the conductivity of the external medium (Weaver and Chizmadzhev 1996; Kotnik et al. 1997). If the cell is modelled as being non-conductive, the value of the external medium conductivity is not important, but must be of non-zero value. The cell was exposed to a homogenous electric field by applying a constant voltage on the two opposite sides of the box, as shown in Fig. 1a. Natural boundary conditions (currents parallel to the side) were applied to the other sides of the box owing to the symmetry of our problem.

The object of our analysis was the electrical potential on the ellipse, obtained in the cross-section of the spheroid with the xz plane, as shown in Fig. 1a. The calculations were performed for different angles of orientation α (0°, 15°, 30°, 45°, 60°, 75° and 90°) between the electric field and the axis of symmetry. For data presentation, the normalized $\Delta\phi_i$ ($\Delta\phi_i/ER_1$ for prolate or ER_2 for oblate) was plotted against the normalized arc length $p(\vartheta)/p(2\pi)$. The arc length $p(\vartheta)$ is an elliptic integral of angle ϑ:

$$p(\vartheta) = \int_0^{\arctan\left[\frac{R_1}{R_2}\tan\vartheta\right]} \sqrt{1 - \left(1 - \left(\frac{R_1}{R_2}\right)^2\right)\sin^2\vartheta}\,\mathrm{d}\vartheta \qquad (3)$$

for a prolate spheroid and:

$$p(\vartheta) = \int_0^{\arctan\left[\frac{R_2}{R_1}\tan\vartheta\right]} \sqrt{1 - \left(1 - \left(\frac{R_2}{R_1}\right)^2\right)\sin^2\vartheta}\,\mathrm{d}\vartheta \qquad (4)$$

for an oblate spheroid, where R_1 and R_2 are the cell radii and ϑ is a polar angle on the spheroid as shown in Fig. 1a.

To determine the area of the cell which is permeabilized, i.e. where the membrane permeability is increased, thus allowing the transport of molecules, the surface of the spheroid exposed to $\Delta\phi$ above $\Delta\phi_c$ was calculated. $\Delta\phi_c$ was defined as the maximum $\Delta\phi_i$ on the membrane of a 40 μm long and 20 μm wide prolate cell for parallel orientation and for a threshold electric field strength 250 V/cm as determined for plated CHO cells (see Fig. 4), which corresponds to 600 mV.

The surface S (surface integral) of the spheroid exposed to a potential difference above the $\Delta\phi_c$ of a prolate or oblate spheroid in spheroidal coordinates τ, φ, σ (see Appendix B) is defined by (Korn and Korn 2000):

$$S = R_2 \int_{\tau_1}^{\tau_2} \int_{\varphi_1}^{\varphi_2} \sqrt{R_1^2(1-\tau^2) + R_2^2\tau^2}\,\mathrm{d}\varphi\,\mathrm{d}\tau \qquad (5)$$

where φ_1, φ_2, τ_1 and τ_2 are borders of integration defined with the condition that $\Delta\phi = \Delta\phi_c$ (see Appendix B).

We validated our numerical model by comparing the results to analytical solutions at different orientations ($\alpha = 0°$, 15°, 30°, 45°, 60°, 75° and 90°) for prolate and oblate shapes. For the whole range of $p(\varphi)$ the largest difference was less than 4%. In Fig. 2, a comparison between numerical (solid lines) calculations and analytical (dashed lines) calculations for an oblate spheroid ($\rho = 5/10$) is shown.

Experimental conditions

Cell treatment

CHO cells were grown in a 10% fetal calf serum complemented MEM medium at 37 °C in Petri dishes. For experiments, 5×10^5 cells were cultured with 2 mL of culture medium in the dishes (35 mm in diameter, Nunc, Denmark) and incubated for 4 h before electrical treatment. At this low density, there was no contact between cells.

Electropermeabilization

Electropulsation was operated using a CNRS cell electropulsator (Jouan, St. Herblain, France), which delivers square-wave electric pulses. The pulse shape was monitored with an oscilloscope (Enertec, St. Etienne, France). A voltage between 80 and 240 V in steps of 20 V was applied on two thin stainless-steel flat and parallel electrodes (10 mm long at 4 mm distance), which corresponds to nominal external electric field intensities between 200 and 600 V/cm in steps of 50 V/cm.

Penetration of propidium iodide (PI) into the cells was used to determine the permeabilization. The culture medium was removed

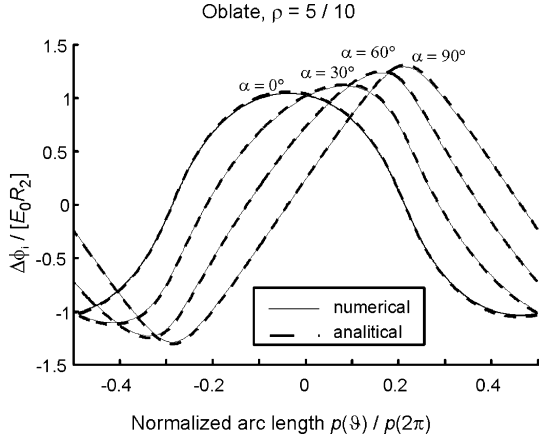

Fig. 2 Comparison of the numerical (*solid lines*) and analytical (*dashed lines*) calculations. Induced transmembrane potential $\Delta\phi_i$ for different angles of orientation α for an oblate spheroid ($\rho = 5/10$) is shown

and replaced by a low ionic content, isoosmolar, pulsing buffer (10 mM phosphate buffer, pH 7.4; 250 mM sucrose, 1 mM $MgCl_2$, $\sigma_o = 0.14$ S m^{-1}) containing 100 μM PI (Sigma). Ten pulses of 5 ms duration at a repetition frequency of 1 Hz were applied at a given electric field intensity at room temperature. These electric field parameters were used in previous studies and gave efficient levels of electropermeabilization, having at the same time relatively good cell viability (Rols and Teissié 1998; Rols et al. 1998b). After application of the pulses the cells were left for 10 min at 30 °C for membrane resealing.

Analysis of the data

The cells were analyzed by fluorescence microscopy. Only the cells between the electrodes which were exposed to the electric pulses were analysed. The percentage of permeabilized cells (i.e. the percentage of fluorescent cells) was determined for different angles of orientation α in steps of 10° from 0° to 90° as a function of the electric field intensity (Fig. 1b). For each electric field intensity, 300 cells were examined on average (which represents 4–6 slides). Duplicate experiments were performed at a 2-day interval. Counts were done in a blind manner by persons who expected no specific results and were not aware of the results of the calculations.

Resting transmembrane potential measurement

Resting transmembrane potential ($\Delta\phi_r$) was determined for plated CHO cells using $DiBac_4(3)$ dye (Molecular Probes, Eugene, Ore., USA). $DiBac_4(3)$ is a slow-response anionic oxonol dye which accumulates in the cytoplasm of depolarized cells in a Nernst equilibrium-dependent way. The Nernst equation can be then resolved using the ratio of fluorescence intensities measured outside (F_{out}) and inside (F_{in}) the cell:

$$\Delta\phi_r = -RT/zF \ln(F_{in}/F_{out}) \quad (6)$$

where R is the gas constant (8.31 J mol^{-1} K^{-1}) and F is Faraday's constant (96,500 C). Determination of F_{in} and F_{out} values was adapted from what was previously described for suspended cells using flow cytometry (Krasznai et al. 1994). Briefly, CHO cells (5×10^5 cells) were grown for 24 h on Lab-Tek II chambered coverglass (Nale Nunc, Naperville, USA). The F_{out} value was determined using chemically fixed and permeabilized cells. Plated cells were washed twice with PBS buffer (138 mM NaCl, 3 mM KCl, 1.5 mM KH_2PO_4, 8 mM NaH_2PO_4, pH 7.4) and incubated for 20 min at 4 °C in a fixation buffer [formaldehyde (2% v/v)- and glutaraldehyde (0.2% v/v)-containing PBS buffer]. Fixed CHO cells were permeabilized at −20 °C for 6 min in absolute methanol. The cells were then washed with PBS and incubated for 3 min in 2 mL of 150 nM $DiBac_4(3)$-containing pulsing buffer. F_{in} was determined using native cells directly incubated in 2 mL of 150 nM $DiBac_4(3)$-containing pulsing buffer, for 3 min. The average intracellular fluorescence levels of fixed and native cells (sampling, $n = 150$) were measured at room temperature, using an ultra-low-light intensifying fluorescence imaging system described previously (Gabriel and Teissié 1998).

Fig. 3 Normalized induced transmembrane potential $\Delta\phi_i/ER_1$ for different angles of orientation α for a prolate spheroid: (**a**) $\rho = 10/2$, (**b**) $\rho = 10/5$ and (**c**) $\rho = 10/8$. *Horizontal lines* represent the threshold values

Results

Theoretical calculations

The induced transmembrane potential $\Delta\phi_i$ was calculated numerically for prolate spheroids with ratios $\rho = 10/8$, 10/5 and 10/2 and for oblate spheroids with ratios $\rho = 8/10$, 5/10 and 2/10 for various angles of cell orientation α with respect to the applied electric field. In Fig. 3 the results for prolate spheroids are presented along an ellipse obtained by a cross-section of the spheroid with the *xz* plane.

In Fig. 3a the normalized maximum $\Delta\phi_i$ for $\rho = 10/2$ drops from 1.06 to 0.37 (i.e. 65%) if the prolate spheroid is rotated from a parallel ($\alpha = 0°$) to a perpendicular ($\alpha = 90°$) orientation. For smaller ratios ρ (i.e. more spherical cells) in Fig. 3b and Fig. 3c, the change of the normalized maximum $\Delta\phi_i$ is smaller and for $\rho = 10/8$ it is from 1.36 to 1.22 (i.e. 10%).

For a given critical transmembrane potential $\Delta\phi_c$ (horizontal lines in Fig. 3) it can be seen that for different orientations also the length of the ellipse and consequentially the area of the spheroid above $\Delta\phi_c$ is changed and this feature is most pronounced at high ρ.

Experimental results

The resting transmembrane potential $\Delta\phi_r$ of sub-confluent plated CHO cells was determined in two independent experiments as the mean of 150 measurements and was −54 mV with a standard deviation ±5 mV at room temperature.

As already observed in many systems, permeabilization of CHO cells was only detected for electric field values higher than a given threshold (Teissié and Rols 1993). This threshold value for plated CHO cells was between 200–250 V/cm (Fig. 4) for pulses of milliseconds in duration. Above this threshold, an increase in the voltage intensity led to an increase in the percentage of permeabilized cells. At 600 V/cm, almost 100% of the plated CHO cells were permeabilized (Fig. 4).

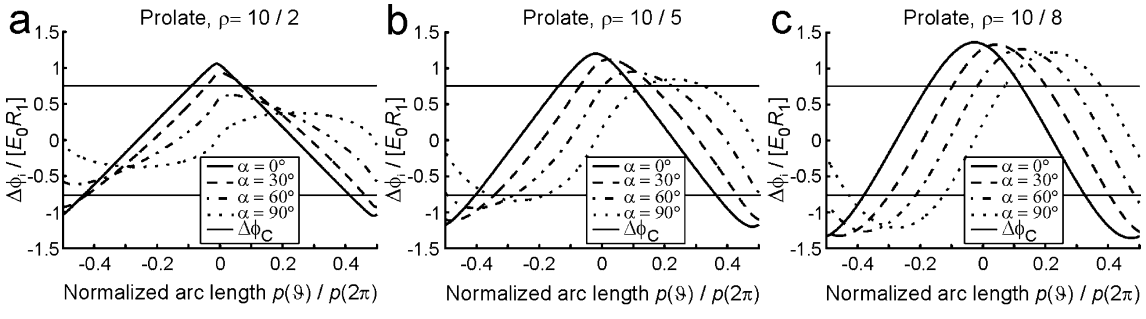

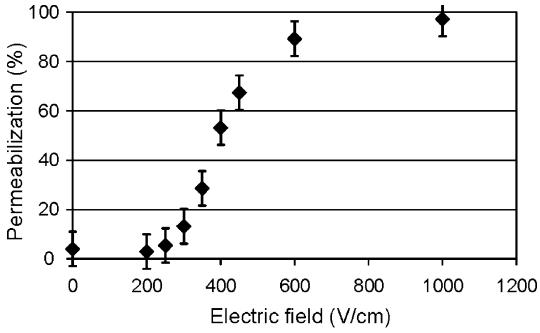

Fig. 4 Electropermeabilization of plated CHO cells as a function of the applied electric field. Ten pulses of 5 ms duration were applied at a 1 Hz repetition frequency at various electric field intensities in the presence of propidium iodide. The percentage of permeabilized cells was determined by fluorescence microscopy

The electric field was increased, above the permeabilization threshold, by steps of 50 V/cm from 200 to 600 V/cm. In Fig. 5, photos of plated CHO cells are given in phase contrast and fluorescence showing the permeabilization for three different electric field intensities. At 350 V/cm, only cells parallel to the electric field (marked with Roman numerals) are permeabilized, while cells perpendicular to the electric field (marked with Arabic numerals) are not (Fig. 5, a and b). At 400 V/cm, the number of permeabilized cells increases, but cells perpendicular to the field are still not permeabilized (Fig. 5, c and d). At 600 V/cm, most cells become permeabilized and the orientation no longer has an effect on the cell permeabilization (Fig. 5, e and f).

Comparison of theoretical and experimental results

In order to compare the theoretical and experimental results, we consider the cell to be permeabilized when the transmembrane potential ($\Delta\phi$) exceeds the critical transmembrane potential ($\Delta\phi_c$). If $\Delta\phi > \Delta\phi_c$, the area of the cell membrane where $\Delta\phi > \Delta\phi_c$ represents the area through which the PI flux is established.

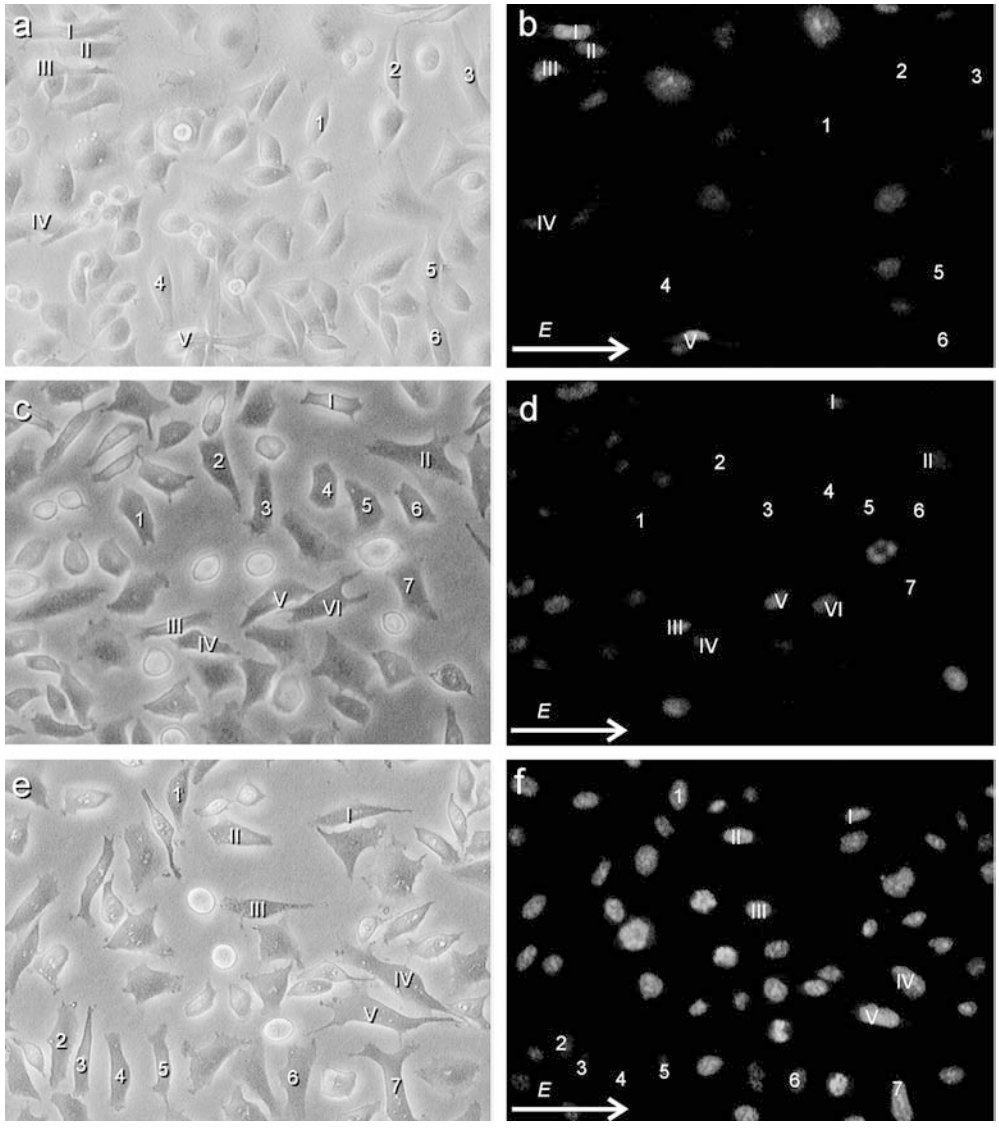

Fig. 5 Visualization of permeabilized CHO cells. The cells have been permeabilized on a culture dish under the microscope by application of 10 pulses (5 ms, 1 Hz frequency) at (**a**, **b**) 350 V/cm, (**c**, **d**) 400 V/cm and (**e**, **f**) 600 V/cm. For (**a**, **c**, **e**) the cells are under phase contrast; for (**b**, **d**, **f**) the cells are under fluorescence. The *arrows* indicate the electric field direction. *Roman numbers* are indicative of cells parallel to the electric field direction; *Arabic numbers* are indicative of cells perpendicular to the electric field direction

$\Delta\phi_c$ was defined as the maximum $\Delta\phi_i$ on the membrane of a 40 μm long and 20 μm wide prolate cell for parallel orientation and for a threshold electric field strength of 250 V/cm, as determined for plated CHO cells (see Fig. 4). The threshold transmembrane potential in vitro, however, is not exactly the same as the maximum $\Delta\phi_i$ on the membrane, because to obtain the permeabilization we have to have a non-zero area exposed to $\Delta\phi$ above $\Delta\phi_c$, so the threshold transmembrane potential in vitro is lower than $\Delta\phi_c$. The value of $\Delta\phi_c$ is 600 mV and it is used in Fig. 6, where the surface of the cell where $\Delta\phi_c$ was exceeded is plotted as a function of the cell orientation angle α and the strength of electric field E. In Fig. 6a, $\Delta\phi_r$ is not taken into account ($\Delta\phi_r = 0$ mV), whereas in Fig. 6b it is taken into account ($\Delta\phi_r = -50$ mV, corresponding to −54 mV measured in plated CHO cells).

In our calculations we considered only a single cell placed in a homogeneous electric field. It was shown previously, however, that for very small distances between the cells ($a \approx R$) the induced transmembrane potential $\Delta\phi_i$ is lower due to interactions between neighbouring cells (Susil et al. 1998; Pavlin et al. 2002). Since under our experimental conditions with a cell density of 5×10^5 cells per 10 cm^2 the cells were not confluent, these interactions between cells were not taken into account.

To correlate the numerical and experimental results we also have to consider that in a population of cells we have a distribution of cell sizes, so some cells are permeabilized below and some above the critical electric field. Thus, the numerically calculated larger area of the cell where $\Delta\phi_c$ was exceeded corresponds to the larger number of permeabilized cells in the experiment. Therefore, the surface of the cell where $\Delta\phi_c$ was exceeded can be correlated to the percentage of permeabilized cells obtained experimentally (Fig. 6c).

Clearly, both the area of the cell with an overcritical $\Delta\phi$ and the permeabilization depend on the electric field intensity and on the angle of orientation α. If the electric field is slightly higher than the threshold, then only cells parallel to the electric field are permeabilized. We observed that, at an applied field between 300 and 450 V/cm, cells oriented parallel to the electric field are predominantly being permeabilized. When the electric field is increased, the cells which are perpendicular to the direction of the field also become permeabilized. For an electric field higher than 500 V/cm the cells become permeabilized irrespective of their orientation with the respect to the electric field.

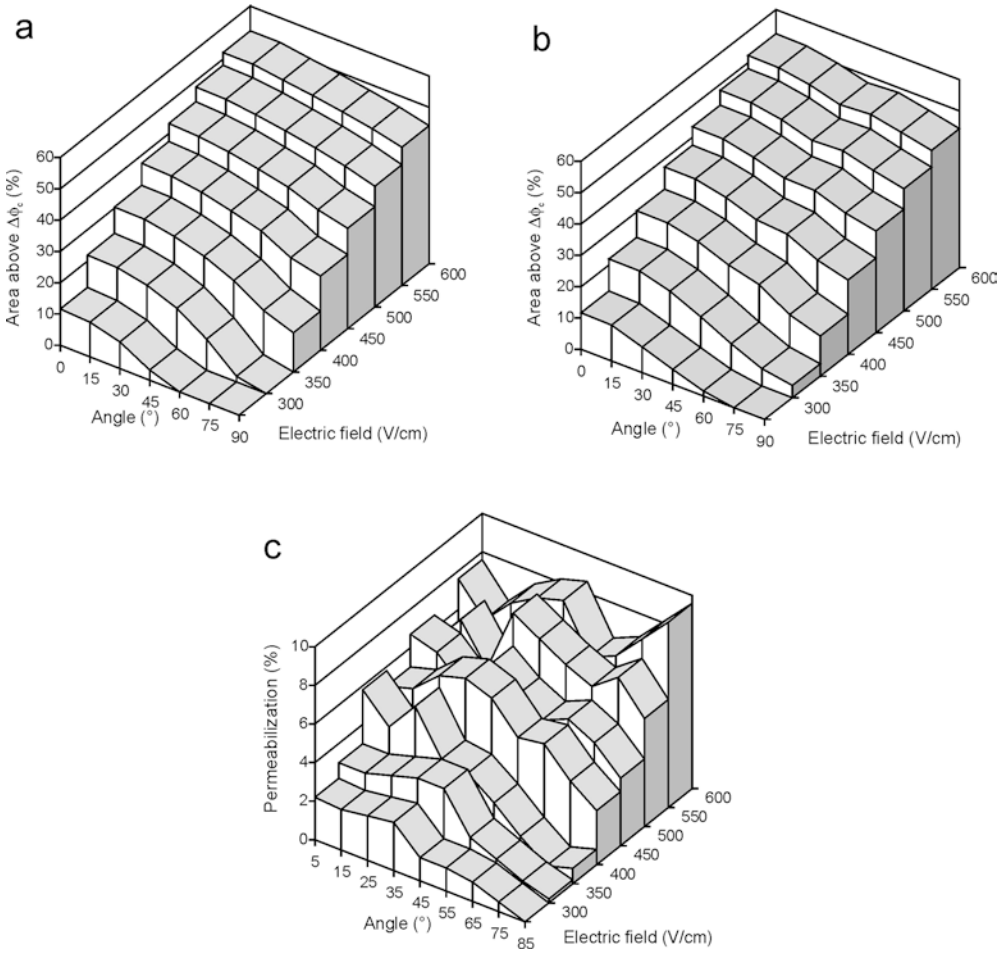

Fig. 6 Comparison of theoretical and experimental results. The cell area above the critical transmembrane potential $\Delta\phi_c$ (**a**, **b**) and electropermeabilization (**c**) for different angles of orientation α is plotted as a function of the applied electric field. **a** Percentage of cell area above $\Delta\phi_c$ for a prolate spheroid having $\rho = 10/5$, corresponding to plated CHO cells; resting transmembrane potential $\Delta\phi_r = 0$ mV. **b** As **a**, but $\Delta\phi_r = -50$ mV, corresponding to plated CHO cells. **c** Percentage of electropermeabilized plated CHO cells

Discussion and conclusion

In this paper, the effect of cell orientation in an electric field on the induced transmembrane potential $\Delta\phi_i$ was analyzed. $\Delta\phi_i$ was calculated for spheroidal cells for different orientations numerically, by using the finite elements method, and analytically. We present an analytical solution for $\Delta\phi_i$ in the form of a generalized Schwan equation for an arbitrary oriented spheroidal cell having a non-conducting membrane, as in Gimsa and Wachner (2001). By comparing our numerical results with analytical calculations, we validated the finite elements method used. The advantage of the numerical approach by the finite elements method is that $\Delta\phi_i$ can be calculated for arbitrary shaped cells, which is not possible analytically. The theoretical results expressed in terms of the area exposed to $\Delta\phi$ above the critical value were compared to experimental results for the electropermeabilization of plated CHO cells.

Theoretical results show that for elongated cells ($\rho >> 1$) the maximum $\Delta\phi_i$ strongly depends on the cell orientation (Fig. 3a). Also, the area of the cell where $\Delta\phi_c$ is exceeded depends on the cell orientation. This area represents the permeabilized surface of the cell membrane through which the transport of molecules occurs.

The $\Delta\phi$ value needed for permeabilization is in the range 200–1000 mV (Weaver and Powell 1989; Teissié and Rols 1993; Eynard et al. 1998; Bier et al. 1999; Miklavčič et al. 2000) and the resting transmembrane potential of the cell is between −20 mV and −70 mV. In general, it is difficult to evaluate the contribution of $\Delta\phi_r$ because it is specific for a given cell line and experimental conditions. For plated CHO cells it was determined to be −54 mV. When $\Delta\phi_r$ was included in our calculations, the difference in results was negligible.

Our in vitro experiments using plated CHO cells show a clear dependence of cell permeabilization on the applied electric field intensity. Moreover, experimental results demonstrate that, for a given electric field intensity, cell permeabilization (i.e. PI uptake) also depends on their orientation with respect to the electric field. Thus for cells of non-spherical shape, their orientation with respect to the electric field also has to be considered. When comparing experimental electropermeabilization results of plated CHO cells (Fig. 6c) with theoretical results for the percentage of the cell area (Fig. 6, a and b), where $\Delta\phi_c$ is exceeded, a good correlation is observed. Furthermore, the theoretical results agree well with experimental results, showing that, for a high enough electric field, no orientation angle dependency is observed. Since in practical use of electropermeabilization, especially for gene transfection, we need to use the electric field high enough to achieve permeabilization but at the same time low enough to keep the viability of the cells, we conclude that the orientation of the cells in the applied electric field is an important parameter.

In contrast to plated cells grown in Petri dishes, cells in suspension can freely rotate. Electroporation of rod-shaped bacteria shows a field-induced orientation phenomenon. Indeed, it was demonstrated previously that the electric pulse must be long enough to orient cells parallel to the field direction in order that these elongated cells become permeabilized (Eynard et al. 1998). These observations agree with our calculations for prolate spheroids, where the maximum $\Delta\phi_i$ is obtained in cells parallel to the applied electric field.

Our results are also in agreement with previous data on plated CHO cell fusion, where it was shown that the maximum fusion yield was obtained using different electric field orientations (Teissié and Blangero 1984). Similarly, it has been demonstrated in previous experiments on tissue permeabilization in vivo that changing the electrode orientation (i.e. field orientation) has an important effect on permeabilization efficiency (Serša et al. 1996). Part of the improvement was ascribed to better coverage of the tumor tissue with a sufficiently high electric field (Šemrov and Miklavčič 1998). An important contribution, however, can be ascribed to the dependence of $\Delta\phi_i$ on field orientation, as demonstrated by our study.

Acknowledgements The authors thank C. Millot for providing CHO cells. M.G. was supported by a grant from the Association Française contre les Myopathies (AFM). This work was partly supported by the Ministry of Education, Science and Sport of the Republic of Slovenia through various grants and partly by the Cliniporator project (grant QLK3-1999-00484) under the framework of the 5th PRCD of the European Commission.

Appendix

Appendix A

In this section, the analytical solution for the induced transmembrane potential $\Delta\phi_i$ on a spheroidal cell is briefly discussed. Under normal physiological conditions the membrane conductance is several orders of magnitude lower than the external medium (Weaver and Chizmadzhev 1996; Kotnik et al. 1997), thus reducing the problem to solving a Laplace equation for a potential ϕ on a surface of a non-conductive spheroid lying in the external electrical field:

$$\Delta\phi(r,\vartheta,\varphi) = 0, \quad j_n \Big|_S = 0 \tag{7}$$

where j_n is the normal component of the electric current at the surface of the spheroid, which for a non-conductive membrane is zero. This is analogous to solving a problem of the potential distribution at the surface of a dielectric spheroid (Stratton 1941). This solution can be extended to the frequency-dependent problem of a spheroid surrounded by a shell having both dielectric and conductive properties, and has been applied to cells by several authors to calculate the frequency-dependent $\Delta\phi_i$ (Schwartz et al. 1965; Bernhardt and Pauly 1973;

Zimmermann et al. 1974; Gimsa and Wachner 2001). The solution for a DC case can be correspondingly obtained by solving the Laplace equation in the spheroidal coordinate system, which for parallel orientation has been given by Kotnik and Miklavčič (2000).

The generalized Schwan equation for an arbitrary oriented ellipsoid can be written as:

$$\Delta\phi_{\mathrm{i}} = \sum_{i=x,y,z} r_i E_i \frac{1}{1-L_i} \tag{8}$$

where the r_i is the vector of the point $T(x, y, z)$ lying at the surface of the ellipsoid and L_i are the depolarizing factors in the x, y and z directions and are dependent only on the geometrical properties of the ellipsoid. The sum of the depolarizing factors is always 1.

Analytical equations for depolarizing factors for an ellipsoid can be found in the paper by Stratton (1941). Here we shall limit ourselves only to an axially symmetrical ellipsoid where $R_1 > R_2 = R_3$ for a prolate spheroid and $R_1 < R_2 = R_3$ for an oblate spheroid. The depolarizing factor for the prolate spheroid along the symmetry axis is:

$$L_z = \frac{1-e^2}{2e^3}\left[\log\frac{1+e}{1-e} - 2e\right], \qquad e = \sqrt{1-(R_2/R_1)^2} \tag{9}$$

and for the oblate spheroid is:

$$L_z = \frac{1}{e^3}\left[e - \sqrt{1-e^2}\arcsin e\right], \qquad e = \sqrt{1-(R_1/R_2)^2} \tag{10}$$

The depolarizing factors in the other two directions can be calculated from the condition that the sum is equal to one:

$$L_x = L_y = \frac{1}{2}(1-L_z) \tag{11}$$

If the z axis of the coordinate system is parallel to the symmetry axis of the spheroid, then the solution for the parallel and perpendicular orientations is:

$$\Delta\phi_{\mathrm{i}_\parallel} = zE\tfrac{1}{1-L_z}, \quad \Delta\phi_{\mathrm{i}_\perp} = xE\tfrac{1}{1-L_x} \tag{12}$$

For a sphere where $R_1 = R_2 = R$, then $L_x = L_y = L_z = 1/3$ and $z = R\cos\vartheta$; thus from Eq. 12 we obtain:

$$\Delta\phi_{\mathrm{i}\parallel} = \Delta\phi_{\mathrm{i}\perp} = \frac{3}{2}RE\cos\vartheta \tag{13}$$

which is the well-known Schwan equation (Eq. 1). See Table 1.

In its most general case the electric field orientation is defined by the angles α (Fig. 1c) and β:

$$\mathbf{E} = \begin{pmatrix} E_x \\ E_y \\ E_z \end{pmatrix} = E\begin{pmatrix} \sin\alpha\cos\beta \\ \sin\alpha\sin\beta \\ \cos\alpha \end{pmatrix} \tag{14}$$

but without loss of generality we can always choose $\beta = 0$ so the vector of the electric field lies in the xz plane. The point $T(x, y, z)$ at the surface of the spheroid in the spherical coordinates can be written as:

$$\mathbf{r} = \begin{pmatrix} x \\ y \\ z \end{pmatrix} = |\mathbf{r}|\begin{pmatrix} \sin\vartheta\cos\varphi \\ \sin\vartheta\sin\varphi \\ \cos\vartheta \end{pmatrix} \tag{15}$$

where the absolute value of $|\mathbf{r}|$ is:

$$|\mathbf{r}| = \frac{1}{\sqrt{\frac{\cos^2\vartheta}{R_1^2} + \frac{\sin^2\vartheta}{R_2^2}}} \tag{16}$$

Introducing Eqs. 14, 15, 16 into Eq. 8, $\Delta\phi_{\mathrm{i}}$ on an arbitrary oriented spheroid for an infinitely small membrane conductance can be obtained:

$$\Delta\phi_{\mathrm{i}} = E\frac{1}{\sqrt{\frac{\cos^2\vartheta}{R_1^2} + \frac{\sin^2\vartheta}{R_2^2}}}\begin{pmatrix} \sin\alpha\cos\beta \\ \sin\alpha\sin\beta \\ \cos\alpha \end{pmatrix}\begin{pmatrix} \frac{1}{1-L_x}\sin\vartheta\cos\varphi \\ \frac{1}{1-L_y}\sin\vartheta\sin\varphi \\ \frac{1}{1-L_z}\cos\vartheta \end{pmatrix} \tag{17}$$

For $\beta = 0$ and presented in the Cartesian coordinate system, the above equation simplifies to:

$$\Delta\phi_{\mathrm{i}} = E\sin\alpha\frac{1}{1-L_x}x + E\cos\alpha\frac{1}{1-L_z}z \tag{18}$$

Table 1 Depolarizing factors L_x, L_y and L_z and normalized maximal induced transmembrane potential $\Delta\phi_{\mathrm{i}}/ER_1$ for an oblate spheroid or $\Delta\phi_{\mathrm{i}}/ER_2$ for a prolate spheroid for different shapes and orientations. For a sphere ($R_1 = R_2$) the normalized induced transmembrane potential is 1.5

Shape	Depolarizing factors			$\Delta\phi_{\mathrm{i,max}}/ER_{1/2}$[a] for different angles of orientation α						
	L_x	L_y	L_z	0°	15°	30°	45°	60°	75°	90°
Prolate, $\rho = 10/8$	0.3620	0.3620	0.2760	1.360	1.351	1.329	1.299	1.266	1.237	1.220
Prolate, $\rho = 10/5$	0.4130	0.4130	0.1740	1.200	1.180	1.120	1.037	0.946	0.873	0.842
Prolate, $\rho = 10/2$	0.4720	0.4720	0.0560	1.056	1.023	0.932	0.790	0.618	0.453	0.375
Oblate, $\rho = 8/10$	0.3030	0.3030	0.3940	1.291	1.305	1.324	1.354	1.380	1.401	1.408
Oblate, $\rho = 5/10$	0.2364	0.2364	0.5272	1.042	1.061	1.111	1.174	1.235	1.279	1.292
Oblate, $\rho = 2/10$	0.1250	0.1250	0.7500	0.789	0.818	0.888	0.976	1.051	1.112	1.132

[a]For a prolate spheroid, $\Delta\phi_{\mathrm{i}}$ is maximal for parallel orientation ($\alpha = 0°$): $\Delta\phi_{\mathrm{i,max}}(\mathrm{prolate}) = \frac{1}{1-L_z}$; for an oblate spheroid, $\Delta\phi_{\mathrm{i}}$ is maximal for perpendicular orientation ($\alpha = 90°$): $\Delta\phi_{\mathrm{i,max}}(\mathrm{oblate}) = \frac{1}{1-L_x}$

This solution is the same as derived by Gimsa and Wachner (2001), only presented in a form that is analogous to the Schwan equation and already taking into account all simplifications that are valid for the cells. Thus from the solution for the induced potential in parallel and perpendicular orientations, one can calculate $\Delta\phi_i$ on an arbitrarily oriented spheroid by means of a linear combination of the two solutions. In other words, in the coordinate system of the spheroid the electric field has two components: in the x and z directions. Since the potential is a linear function, we can simply add the potential induced in the perpendicular direction and the one induced in the parallel direction.

Appendix B

For the calculation of the area where the critical transmembrane potential $\Delta\phi_c$ is exceeded, we have to integrate the surface on the spheroid in spheroidal coordinates τ, φ and σ (Korn and Korn 2000). The transformation from Cartesian coordinates to spheroidal coordinates for a prolate spheroid is defined by:

$$\begin{aligned} x^2 &= \left(R_1^2 - R_2^2\right)\left(\sigma^2 - 1\right)\left(1 - \tau^2\right)\cos^2\varphi \quad \sigma > 1 \\ y^2 &= \left(R_1^2 - R_2^2\right)\left(\sigma^2 - 1\right)\left(1 - \tau^2\right)\sin^2\varphi \quad 0 < \varphi < 2\pi \\ z &= \sqrt{R_1^2 - R_2^2}\,\sigma\tau \quad -1 < \tau < 1 \end{aligned} \tag{19}$$

and for oblate spheroid by:

$$\begin{aligned} x^2 &= \left(R_2^2 - R_1^2\right)\left(\sigma^2 + 1\right)\left(1 - \tau^2\right)\cos^2\varphi \quad \sigma > 0 \\ y^2 &= \left(R_2^2 - R_1^2\right)\left(\sigma^2 + 1\right)\left(1 - \tau^2\right)\sin^2\varphi \quad 0 < \varphi < 2\pi \\ z &= \sqrt{R_2^2 - R_1^2}\,\sigma\tau \quad -1 < \tau < 1 \end{aligned} \tag{20}$$

The surface element in spheroidal coordinates is (Korn and Korn 2000):

$$\mathrm{d}S = \sqrt{g_{\varphi\varphi} g_{\tau\tau}}\,\mathrm{d}\varphi\,\mathrm{d}\tau \tag{21}$$

where $g_{\varphi\varphi}$ and $g_{\tau\tau}$ are elements of the metric tensor in spheroidal coordinates.

The equation of the surface of the spheroid is:

$$S = R_2 \int_{\tau_1}^{\tau_2} \int_{\varphi_1}^{\varphi_2} \sqrt{R_1^2(1 - \tau^2) + R_2^2\tau^2}\,\mathrm{d}\varphi\,\mathrm{d}\tau \tag{22}$$

where φ_1, φ_2, τ_1 and τ_2 are borders of integration defined by the condition that $\Delta\phi_i = \Delta\phi_c$. As already mentioned, we analyzed $\Delta\phi_i$ on an ellipse, obtained from the cross-section of a spheroid with the xz plane. For two points on the ellipse where $\Delta\phi_c$ was exceeded, an ellipse on a spheroid through these two points can also be defined, which is perpendicular to plane xz. This ellipse represents our border of integration. The border of integration where $\Delta\phi_c$ has been exceeded is a closed curve on an ellipsoid which is nearly an ellipse. By transforming this ellipse into spheroidal coordinates, the φ_1, φ_2, τ_1 and τ_2 values are obtained.

References

Bernhardt J, Pauly H (1973) On the generation of potential differences across the membranes of ellipsoidal cells in an alternating electrical field. Biophysik 10:89–98

Bier M, Hammer SM, Canaday DJ, Lee RC (1999) Kinetics of sealing for transient electropores in isolated mammalian skeletal muscle cells. Bioelectromagnetics 20:194–201

Brock TD, Smith DW, Madigan MT (1984) Biology of microorganisms. Prentice-Hall, Engelwood Cliffs, NJ, USA

Eynard N, Rodriguez F, Trotard J, Teissié J (1998) Electrooptics studies of *Escherichia coli* electropulsation: orientation, permeabilization, and gene transfer. Biophys J 75:2587–2596

Fear CE, Stuchly MA (1998) Modeling assemblies of biological cells exposed to electric eields. IEEE Trans Biomed Eng 45:1259–1271

Fricke H (1925) A mathematical treatment of the electrical conductivity and capacity of disperse systems. II. The capacity of conducting spheroids surrounded by a non-conducting membrane for a current of low frequency. Phys Rev 26:678

Gabriel B, Teissié J (1998) Fluorescence imaging in the millisecond time range of membrane electropermeabilisation of single cells using a rapid ultra-low-light intensifying detection system. Eur Biophys J 27:291–298

Gimsa J, Wachner D (2001) Analytical description of the transmembrane voltage induced on arbitrarily oriented ellipsoidal and cylindrical cells. Biophys J 81:1888–1896

Hart FX, Marino AA (1982) ELF dosage in ellipsoidal model of men due to high voltage transmission lines. J Bioelec 1:129–154

Korn GA, Korn TM (2000) Mathematical handbook for scientists and engineers. Dover, Mineola, NY, USA

Kotnik T, Miklavčič D (2000) Analytical description of transmembrane voltage induced by electric fields on spheroidal cells. Biophys J 79:670–679

Kotnik T, Bobanović F, Miklavčič D (1997) Sensitivity of transmembrane voltage induced by applied electric fields: a theoretical analysis. Bioelectrochem Bioenerg 43:285–291

Krasznai Z, Marian T, Balkay L, Emri M, Tron L (1994) Flow cytometric determination of absolute membrane potential of cells. J Photochem Photobiol 28:93–99

Miklavčič D, Šemrov D, Mekid H, Mir LM (2000) A validated model of in vivo electric field distribution in tissues for electrochemotherapy and for DNA electrotransfer for gene therapy. Biochim Biophys Acta 1523:73–83

Miller CE, Henriqez CS (1988) Three-dimensional finite element solution for biopotentials: erythrocyte in an applied field. IEEE Trans Biomed Eng 35:712–718

Mir LM (2001) Therapeutic perspectives of in vivo cell electropermeabilization. Bioelectrochemistry 53:1–10

Neumann E (1989) The relaxation hysteresis of membrane electroporation. In: Neumann E, Sowers AE, Jordan CA (eds) Electroporation and electrofusion in cell biology. Plenum, New York, pp 61–82

Neumann E, Schaefer-Ridder M, Wang Y, Hofschneider PH (1982) Gene transfer into mouse lyoma cells by electroporation in high electric fields. EMBO J 1:841–845

Pavlin M, Pavšelj N, Miklavčič D (2002) Dependence of induced transmembrane potential on cell density, arrangement, and cell position inside the cell system. IEEE Trans Biomed Eng 49:605–612

Rols MP, Teissié J (1998) Electropermeabilization of mammalian cells to macromolecules: control by pulse duration. Biophys J 75:1415–1423

Rols MP, Delteil C, Golzio M, Dumond P, Cros S, Teissie J (1998a) In vivo electrically mediated protein and gene transfer in murine melanoma. Nat Biotechnol 16:168–171

Rols MP, Delteil C, Golzio M, Teissié J (1998b) In vitro and ex vivo electrically mediated permeabilization and gene transfer in murine melanoma. Bioelectrochem Bioenerg 47:129–134

Satkauskas S, Bureau MF, Puc M, Mahfoudi A, Scherman D, Miklavcic D, Mir LM (2002) Mechanisms of in vivo DNA electrotransfer: respective contributions of cell electropermeabilization and DNA electrophoresis. Mol Ther 5:133–140

Schwan HP (1957) Electrical properties of tissue and cell suspensions. Adv Biol Med Phys 5:147–209

Schwarz G, Saito M, Schwan HP (1965) On the orientation of nonspherical particles in an alternating electrical field. J Chem Phys 10:3562–3569

Šemrov D, Miklavčič D (1998) Calculation of the electrical parameters in electrochemotherapy of solid tumours in mice. Comput Biol Med 28:439–448

Serša G, Čemažar M, Šemrov D, Miklavčič D (1996) Changing electrode orientation improves the efficacy of electrochemotherapy of solid tumors in mice. Bioelectrochem Bioenerg 39:61–66

Sillars RW (1937) The properties of dielectrics containing semiconducting particles various shapes. J Inst Elec Eng 80:378–394

Stratton JA (1941) Electromagnetic theory. McGraw-Hill, New York

Sukharev SI, Klenchin VA, Serov SM, Chernomordik LV, Chizmadzhev YA (1992) Electroporation and electrophoretic DNA transfer into cells. The effect of DNA interaction with electropores. Biophys J 63:1320–1327

Susil R, Šemrov D, Miklavčič D (1998) Electric field-induced transmembrane potential depends on cell density and organization. Elec Magnetobiol 17:391–399

Teissié J, Blangero C (1984) Direct experimental evidence of the vectorial character of the interaction between electric pulses and cells in cell electrofusion. Biochim Biophys Acta 775:446–448

Teissié J, Rols MP (1993) An experimental evaluation of the critical potential difference inducing cell membrane electropermeabilization. Biophys J 65:409–413

Tekle E, Astumian RD, Chock PB (1990) Electro-permeabilization of cell membranes: effect of the resting membrane potential. Biochem Biophys Res Commun 172:282–287

Weaver JC, Chizmadzhev YA (1996) Electroporation. In: Polk C, Postow E (eds) Biological effects of electromagnetic fields. CRC, Boca Raton, Fla., USA, pp 247–274

Weaver JC, Powell KT (1989) Theory of electroporation. In: Neumann E, Sowers AE, Jordan CA (eds) Electroporation and electrofusion in cell biology. Plenum, New York, pp 111–112

Zimmermann U (1982) Electric field-mediated fusion and related electrical phenomena. Biochim Biophys Acta 694:227–277

Zimmermann U, Pilwat G, Riemann F (1974) Dielectric breakdown of cell membranes. Biophys J 14:881–899